Biosci. Rep. (2016) / **36** / art:e00402 / doi 10.1042/BSR20160381

Original Paper

OPEN ACCESS

Hepatic glucose utilization in hepatic steatosis and obesity

Georgia Keramida*, James Hunter* and Adrien Michael Peters†[1]

*Clinical Imaging Sciences Centre, Brighton and Sussex Medical School, Brighton BN1 9PX, U.K.
†Division of Clinical and Laboratory Investigation, Brighton and Sussex Medical School, Brighton BN1 9PX, U.K.

Synopsis

Hepatic steatosis is associated with obesity and insulin resistance. Whether hepatic glucose utilization rate (glucose phosphorylation rate; MRglu) is increased in steatosis and/or obesity is uncertain. Our aim was to determine the separate relationships of steatosis and obesity with MRglu. Sixty patients referred for routine PET/CT had dynamic PET imaging over the abdomen for 30 min post-injection of F-18-fluorodeoxyglucose (FDG), followed by Patlak–Rutland graphical analysis of the liver using abdominal aorta for arterial input signal. The plot gradient was divided by the intercept to give hepatic FDG clearance normalized to hepatic FDG distribution volume (ml/min per 100 ml) and multiplied by blood glucose to give hepatic MRglu (μmol/min per 100 ml). Hepatic steatosis was defined as CT density of $\leqslant$40 HU measured from the 60 min whole body routine PET/CT and obesity as body mass index of $\geqslant$30 kg/m^2. Hepatic MRglu was higher in patients with steatosis (3.3 ± 1.3 μmol/min per 100 ml) than those without (1.7 ± 1.2 μmol/min per 100 ml; $P < 0.001$) but there was no significant difference between obese (2.5 ± 1.6 μmol/min per 100 ml) and non-obese patients (2.1 ± 1.3 μmol/min per 100 ml). MRglu was increased in obese patients only if they had steatosis. Non-obese patients with steatosis still had increased MRglu. There was no association between MRglu and chemotherapy history. We conclude that MRglu is increased in hepatic steatosis probably through insulin resistance, hyperinsulinaemia and up-regulation of hepatic hexokinase, irrespective of obesity.

Key words: F-18-fluorodeoxyglucose (FDG), hepatic glucose utilization, hepatic steatosis, liver, PET/CT.

Cite this article as: Bioscience Reports (2016) **36**, e00402, doi:10.1042/BSR20160381

INTRODUCTION

Recent interest in the hepatic accumulation of the glucose radiotracer, F-18-fluorodeoxyglucose (FDG), has focused on three issues: firstly, the validity of using the steatotic liver as a reference region for tumour FDG uptake in PET/CT [1–5]; secondly, the possible use of FDG PET/CT to diagnose hepatic inflammation, especially non-alcoholic steatohepatitis (NASH) [5,6] and thirdly, the determinants of hepatic glucose utilization (MRglu; i.e. hepatic phosphorylation rate of glucose to glucose-6-phosphate via hexokinase; transport constant k_3; Figure 1), especially in hepatic steatosis, insulin resistance and metabolic syndrome [7–9].

Choi et al. [7] were the first to use FDG PET to study hepatic glucose kinetics. They showed a dramatic increase in MRglu (metabolic rate for glucose) following acute administration of glucose in healthy subjects, an increase that was presumably mediated by insulin acting on hepatic hexokinase (k_3). Iozzo et al. [8], employing the euglycaemic hyperinsulinaemic clamp, confirmed that insulin increases hepatic phosphorylation of FDG to FDG-6-phosphate (FDG-6-P). Interestingly, they showed that the increase in k_3 in response to hyperinsulinaemia was at least as marked in patients with low insulin sensitivity as in healthy sedentary subjects (normal insulin sensitivity) and athletes (high insulin sensitivity), suggesting that k_3 remains sensitive to insulin in patients with insulin resistance. In contrast, the dephosphorylation rate of FDG-6-P by glucose-6-phosphatase (k_4) was very slow and insensitive to hyperinsulinaemia in patients with reduced insulin sensitivity.

Insulin resistance is strongly associated with obesity, type 2 diabetes mellitus and hepatic steatosis [10–16]. Patients with insulin resistance have raised blood insulin levels [17]. It is therefore surprising that Borra et al. [9] subsequently found hepatic glucose uptake to correlate *inversely* with hepatic steatosis in patients with type 2 diabetes and to be higher in normal subjects compared with type 2 diabetics.

Abbreviations: FDG, F-18-fluorodeoxyglucose; FDG-6-P, FDG-6-phosphate; NAFLD, non-alcoholic fatty liver disease; NASH, non-alcoholic steatohepatitis; ROI, regions of interest.

[1] To whom correspondence should be addressed (email a.m.peters@bsms.ac.uk).

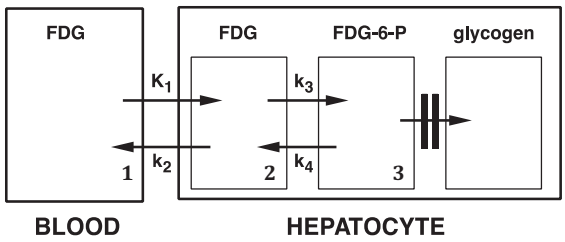

Figure 1 Model of FDG kinetics with reference to the liver

K_1 is hepatic blood flow, k_2 is a diffusion constant, k_3 is hexokinase and k_4 is glucose-6-phosphatase. FDG is assumed to mix throughout its intrahepatic distribution volume (compartments 1 and 2) via K_1 and k_2 by 2 min post-injection. De-phosphorylation (via k_4) in compartment 3 is assumed to be slow enough to ignore. Patlak–Rutland analysis therefore measures k_3.

Although an association between obesity, hepatic steatosis and insulin resistance is well established, how the three conditions are linked remains uncertain. There is strong evidence to suggest that insulin resistances and hepatic steatosis are driven by obesity-induced adipokines [18]. However, not all patients with hepatic steatosis are obese and not all obese patients have hepatic steatosis [19,20]. No previous study has separated the relationships of obesity and hepatic steatosis with MRglu. The purpose of the present study therefore was to examine the relationship between hepatic steatosis and MRglu and determine the separate relationships of obesity and hepatic steatosis with MRglu.

MATERIALS AND METHODS

Patients

Sixty patients (47 men, age range 28–84, and 13 women, age range 40–67) having routine, clinical PET/CT, mostly for the management of cancer, were prospectively recruited for the study. These patients formed the population for a study on a separate issue concerning signal-to-noise ratio in PET published elsewhere [21]. They were classified as obese if body mass index was $\geqslant$30 kg/m^2 and as having hepatic steatosis if CT density was $\leqslant$40 HU [22], as determined from the CT component of their clinical PET/CT study. Twelve had metabolically active lymphoma, 8 had inactive lymphoma, 26 had FDG-avid non-haematological malignancy and 14 more had normal PET/CT. Twelve had received chemotherapy within 6 months of their scan, 19 had received chemotherapy >6 months previously (range 8 months to 10 years) and 29 patients had received no previous chemotherapy (chemotherapy-naïve). Five patients had type 2 diabetes mellitus. There were none with type 1 diabetes mellitus. Patients with known or suspected high ethanol intake were not included. There were a total of 16 patients with no FDG avid malignancy, no hepatic steatosis and no recent chemotherapy, considered to be 'almost normal'. Ethical approval was given by a National Research Ethics Committee and all patients gave written informed consent.

Imaging

Patients fasted for 6 h. Blood glucose was measured immediately before FDG injection using a glucometer (ACCU-CHEK Performa; Inform ll strips; Roche). Prior to routine whole body imaging, dynamic PET imaging was performed following i.v. injection of 400 MBq ($\pm$10 %) FDG, acquiring 30 $\times$ 1 min frames, using a Siemens Biograph 64-slice 16 Truepoint PET/CT scanner (Erlangen, Germany). Following the dynamic study, the patient had routine PET/CT at 60 min post-injection; 3D emission data were acquired at 3 min per bed position (PET reconstruction: four iterations; subset 8; Gaussian pre-filter; FWHM 5 mm; matrix size 168 $\times$ 168; zoom 1).

Image analysis

Hepatic clearance was measured from the dynamic data using Patlak–Rutland analysis. Using *Hermes* software (HERMES), liver activity was summed from regions of interest (ROI) of 3 cm diameter each on approximately 20 transaxial images, avoiding any suspected focal pathology in each transaxial image. Blood pool activity was obtained from ROIs of 1.6 cm diameter carefully placed within the wall of the abdominal aorta in each of approximately 20 transaxial images. Other workers have validated the use of the abdominal aorta for Patlak–Rutland analysis [23,24], including the liver [23].

Patlak–Rutland graphical analysis

After correction for physical decay of F-18, the ratio of hepatic-to-aortic counts/frame was plotted against the ratio of integral of aortic counts-to-aortic counts/frame (Figure 2). The latter ratio has units of time ('normalized time'). The gradient of the plot is proportional to hepatic FDG clearance (Ki) and the intercept is proportional to the distribution volume of un-phosphorylated FDG throughout the liver ($V(0)$) with the same proportionality constant (see Appendix A). Ki was divided by $V(0)$ to give hepatic FDG clearance per unit FDG hepatic distribution volume. In healthy liver, $V(0)$ is almost unity [7,8,25], indicating that FDG rapidly penetrates not only the hepatic interstitial space but also hepatocytes. Ki/$V(0)$ is therefore effectively FDG clearance per unit volume of lean liver and, according to standard equations linking K_1, k_2, k_3, k_4, Ki and $V(0)$, is equal to k_3 [7,8,25]. FDG does not penetrate hepatic fat, the presence of which consequently physically dilutes the FDG signal [26]. Hepatic fat may account for up to 30 % of the liver (equivalent to CT density of $\sim$5 HU [26]) in which case hepatic FDG clearance measured as Ki would underestimate clearance into lean liver by 30 %. Moreover, the distribution of hepatic fat is heterogeneous [27]. Expressing clearance as Ki/$V(0)$ is therefore desirable for determining the relationship between hepatic MRglu and hepatic steatosis. Ki/$V(0)$ was multiplied by the blood glucose concentration (μmol/ml) to give MRglu in units of μmol/min per 100 ml, where 100 ml represents 100 ml fat-free liver. We assumed a lumped constant of unity [28].

Patlak–Rutland analysis is valid when transport of tracer is unidirectional along a single transport pathway. Mixing of FDG

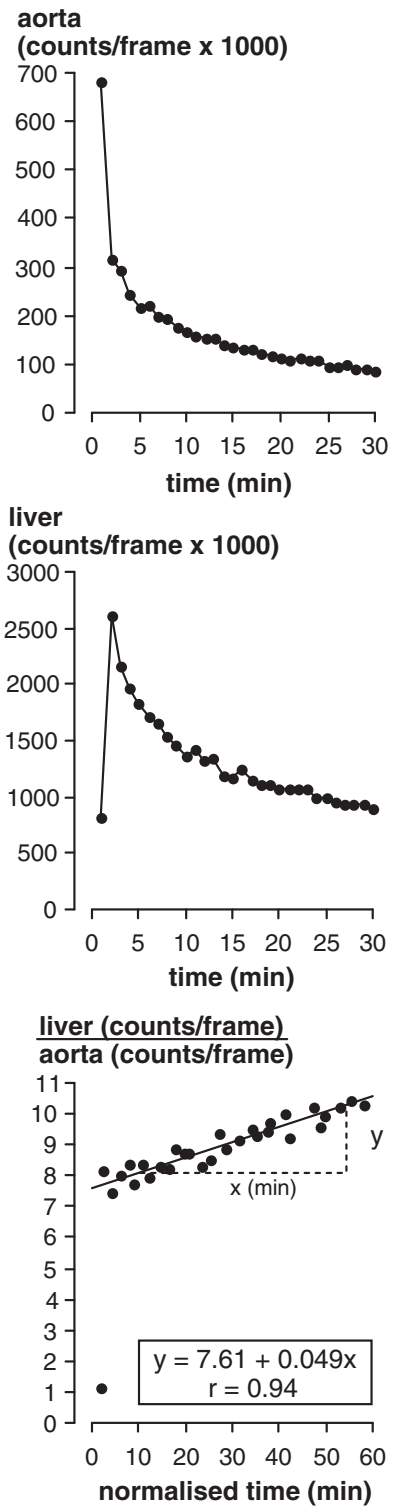

Figure 2 Examples of time compared with counts/frame curves for the aortic blood pool (top), liver (middle) and Patlak–Rutland plot based on these curves (bottom)

Note that the gradient of the plot ($\Delta y/\Delta x$) is proportional to FDG clearance with the same proportionality constant as that relating the intercept to the distribution volume.

between intrahepatic blood and hepatocytes (compartments 1 and 2, Figure 1) is rapid because K_1 and k_2 are high [7,8,25]. Conversely, the de-phosphorylation rate of FDG-6-P via glucose-6-phosphatase appears to be very slow [8,25]. So the only effective transport constant is k_3, which reflects the clearance of FDG by conversion to FDG-6-P.

Mixing of FDG between compartments 1 and 2 was assumed to have been completed within 2 min of FDG injection so the first 2 frame values were not included in the Patlak–Rutland plot. Inspection of the plots revealed that they were essentially linear from 3 to 30 min (Figure 2), consistent with this assumption. This mixing time may seem short but is consistent with previously reported values of K_1 and k_2, which respectively range from 0.01 to 0.015 and 0.013 to 0.016 s^{-1} [7,8,25], and which therefore give an equilibration rate constant of 0.023–0.031 s^{-1}. This gives a time to 95% equilibration of FDG between compartments 1 and 2 of 97–130 s. Munk et al. [25] also obtained Patlak–Rutland plots that were linear within a very few minutes of injection.

Statistical analysis

Normal distributions of data were confirmed using the Shapiro–Wilk test, so parametric statistics were used. Values were expressed as mean ± S.D. Correlations were quantified using Pearson's analysis. Significance of differences between patient groups was tested using Student's unpaired *t* test.

RESULTS

Patient demographics are briefly summarized in Table 1.

Effect of chemotherapy

Mean CT density in 29 chemotherapy-naïve patients was 46 ± 9 HU compared with 43 ± 9 HU in 12 with a history of recent chemotherapy ($P = 0.33$). Patients with distant chemotherapy had a mean CT density of 47 ± 11 HU ($P = 0.8$ compared with chemotherapy-naïve patients). Corresponding values of BMI were 28 ± 5, 28 ± 8 and 26 ± 4 kg/m^2 ($P > 0.1$). There was no significant difference in MRglu between patients with recent chemotherapy (2.6 ± 1.3 μmol/min per 100 ml) and chemotherapy-naïve patients (2.3 ± 1.4 μmol/min per 100 ml; $P = 0.52$).

Prevalence of hepatic steatosis in obese and non-obese patients

CT density correlated inversely with BMI (CT density = 69–0.83*BMI; $r = 0.49$; $P = 0.0001$; Figure 3). Of the 60 patients, 19 (32%) had steatosis and 18 (30%) were obese. Thirty-four had neither steatosis nor obesity, whereas 11 had both. Of the 19 with steatosis, 8 (42%) were not obese, whereas of the 18 who were obese, 11 (61%) had steatosis (Table 1).

Table 1 Patient demographics (±S.D. where indicated)

	CT density (HU)		BMI (kg/m²)	
	⩽40	>40	<30	⩾30
Male/female	16/3	32/9	32/10	16/2
Age (years)	60 ± 13	60 ± 12	62 ± 12	57 ± 13
Blood glucose (mmol/l)	6.4 ± 1.5	5.7 ± 0.6	6.3 ± 1.5	5.7 ± 0.7
Obese/non-obese	11/8	7/34	–	–
Steatosis/no steatosis	–	–	8/34	11/7
PET FDG-avid/non-avid	13/6	21/20	23/20	11/6

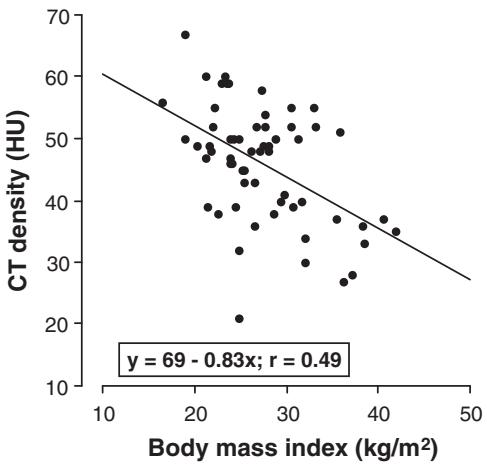

Figure 3 Relationship between CT density and BMI in all patients

Blood glucose levels

Blood glucose levels were slightly but significantly higher in patients with steatosis (6.4 ± 1.5 mmol/l) compared with those without (5.7 ± 0.6 mmol/l; $P = 0.012$) and in obese subjects (6.3 ± 1.5 mmol/l) compared with non-obese (5.7 ± 0.7 mmol/l; $P = 0.035$; Table 1).

Hepatic FDG clearance and MRglu

Liver and aortic blood pool time-activity curves followed similar time courses (Figure 2). Relative to the intercept, Patlak–Rutland analysis of dynamic hepatic and aortic blood pool activity therefore generated fairly shallow positive gradients that appeared to be essentially linear from 3 to 30 min.

Mean MRglu in the almost normal 16 patients was 1.6 ± 1.2 μmol/min per 100 ml. In all 60 patients, there were strong negative correlations between CT density and FDG clearance ($r = -0.52$; $P < 0.0001$) and between CT density and MRglu ($r = -0.56$; $P < 0.0001$; Figures 4 and 5). In contrast, BMI correlated weakly but significantly with MRglu ($r = 0.32$; $P = 0.013$) and showed an insignificant correlation with clearance ($r = 0.21$; $P = 0.11$).

Consistent with the above correlations, MRglu was higher in patients with steatosis (3.3 ± 1.3; $n = 19$) than in those without (1.7 ± 1.2; $n = 41$; $P < 0.001$) but the difference between obese (2.5 ± 1.6; $n = 18$) and non-obese patients (2.1 ± 1.3; $n = 42$) was not significant ($P = 0.2$) (Figure 6). There was no significant difference in MRglu between 8 non-obese (2.9 ± 1.4) and 11 obese (3.5 ± 1.1) patients with steatosis ($P = 0.27$) (Figure 7). However, MRglu in these 11 obese patients with steatosis was higher than in 7 obese patients without steatosis (0.8 ± 0.7; $P < 0.001$). Similar results were obtained with respect to FDG clearance instead of MRglu (Figures 6 and 7). Thus, clearances were 0.51 ± 0.16 ml/min per 100 ml in steatosis compared with 0.30 ± 0.21 ml/min per 100 ml in patients without steatosis ($P < 0.001$) and 0.39 ± 0.23 ml/min per 100 ml in obese patients compared with 0.36 ± 0.21 ml/min per 100 ml in non-obese patients ($P = 0.62$).

Of five patients with type 2 diabetes mellitus, four, all with steatosis (CT densities: 36, 37, 37 and 38 HU), had high values of FDG clearance (0.57 ± 0.11 ml/min per 100 ml) and MRglu (4.5 ± 1.3 μmol/min per 100 ml). In contrast, one patient without steatosis (CT density 50 HU) had low values (0.13 ml/min per 100 ml and 0.8 μmol/min per 100 ml respectively).

DISCUSSION

Hepatocytes, but not other cells, contain glucose-6-phosphatase, which de-phosphorylatesglucose-6-phosphate and FDG-6-P via pathway k_4 (Figure 1). In the fasting state, hepatic glucose production exceeds hepatic glucose uptake as a result of hepatic glycogenolysis and the production of glucose-6-phosphate, thereby maintaining the blood glucose level. FDG, however, is not incorporated into glycogen so the hepatic FDG-6-P concentration depends on the balance of k_3 and k_4. Based on modelling of hepatic FDG kinetics, k_4 has been shown to be low [8] or indeterminate [7] in the fasting state. Dephosphorylation of FDG-6-P is therefore slow and this is compounded by the relatively long time required, via hexokinase, to generate sufficient phosphorylated FDG for k_4 to be clearly detectable. FDG clearance and MRglu are therefore effectively determined by k_3. Previous studies using Patlak–Rutland analysis to measure hepatic glucose utilization rate [8,9,25] recorded linear plots, as we have done, confirm-

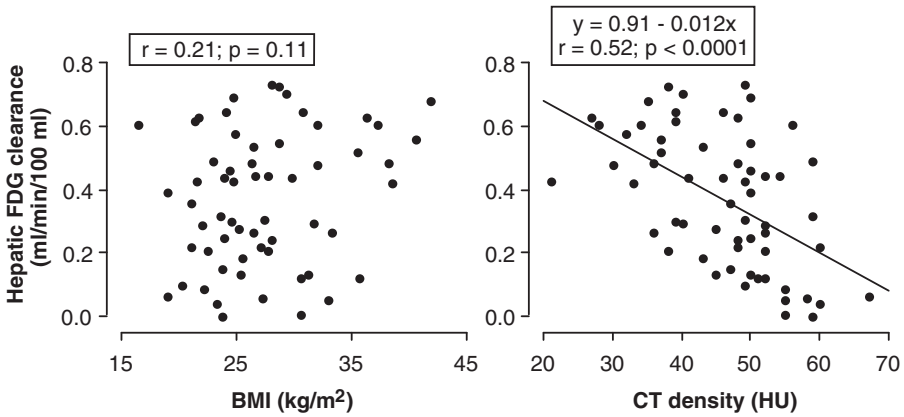

Figure 4 Relations of hepatic FDG clearance with BMI (left panel) and CT density (right panel)

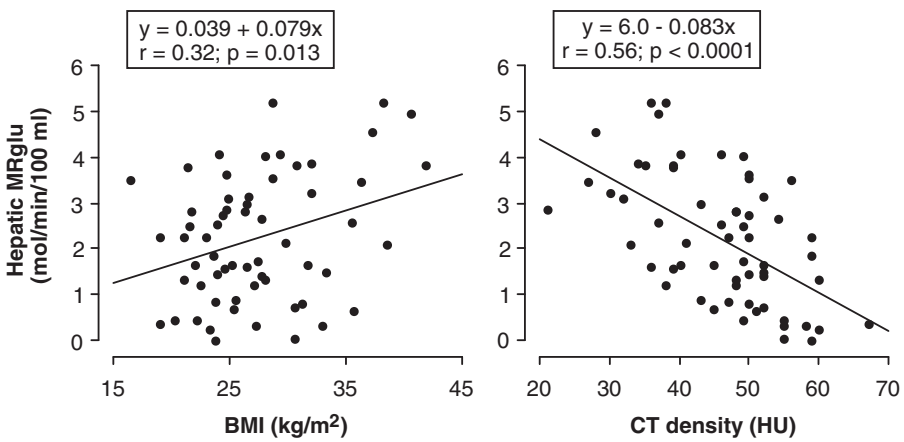

Figure 5 Relations of hepatic glucose utilization rate (MRglu) with BMI (left panel) and CT density (right panel)

ing a very low rate of FDG de-phosphorylation. Moreover, these studies found Patlak–Rutland analysis to be robust for measuring MRglu and independent of errors arising from the liver's dual blood supply that complicate measurement of the transport constants using modelling [25,29].

We measured MRglu by multiplication with blood glucose rather than plasma glucose. Ki and $V(0)$ are lower when based on plasma sampling than whole blood but Ki/$V(0)$ is the same. However, the distribution ratio of FDG between erythrocytes and plasma exceeds 0.8 [30] and plasma glucose is only approximately 10% higher than blood glucose. This means that plasma FDG clearance is only approximately 10% lower than blood clearance and $V(0)$ based on plasma sampling is similarly less than when derived from blood sampling. To compare our values of MRglu with literature values, we need therefore to take into account that previous studies expressed Ki as blood clearance and some as plasma clearance. We also need to take into account that previous studies expressed Ki in terms of total liver volume, including fat. Notwithstanding these limitations, our mean value of MRglu in almost healthy patients of 1.6 μmol/min per 100 ml is similar to values in healthy subjects reported by Choi et al. [7] (2.1 μmol/min per 100 ml; $n = 10$) and Iozzo et al. [8] (1.3 μmol/min per 100 ml; $n = 16$), but less than that of Borra et al. [9] who obtained a mean value in eight healthy subjects of 3.6 μmol/min per100 ml. Choi et al. [7] found $V(0)$ to be 0.88 ml/g in healthy subjects, both fasting and after a glucose load, whereas Iozzo et al. recorded a value in healthy subjects of ~0.8 ml/ml. $V(0)$, however, will be lower in hepatic steatosis because fat will increase V relative to $V(0)$. Interestingly, in the study of Iozzo et al. [8], $V(0)$ was lower in subjects with low insulin sensitivity, 0.75 ml/ml, perhaps because they had higher hepatic fat burden. Munk et al. [25] performed Patlak–Rutland analysis in pigs and obtained $V(0)$ of 1.05 ml/ml but they appeared to count whole blood rather than plasma.

Dividing Ki by $V(0)$ has the advantage that it reflects MRglu in terms of lean hepatic volume and avoids the issues of

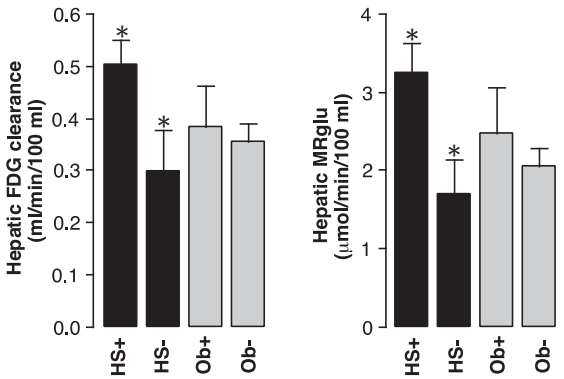

Figure 6 Hepatic FDG clearance and MRglu are increased in patients with hepatic steatosis (HS+) compared with those without (HS−)

In contrast, there are no significant differences between obese (Ob+) and non-obese (Ob−) patients (*$P < 0.001$; bars = S.E.M.).

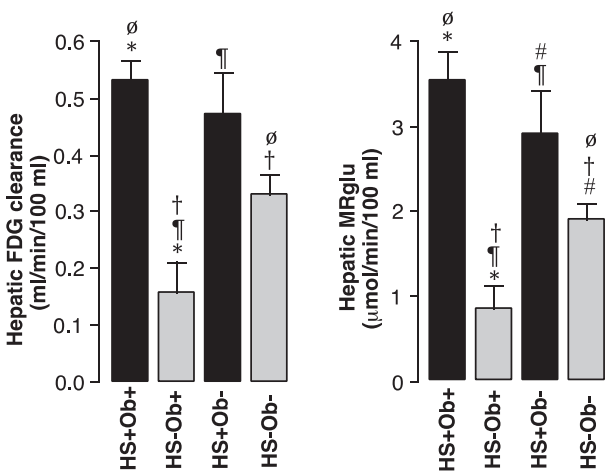

Figure 7 Hepatic FDG clearance and MRglu are increased in patients with steatosis (HS+) whether or not they are obese (Ob+)

In contrast, obese patients only have increased clearance and MRglu when they also have steatosis (*$P < 0.001$; ø$P < 0.01$; ¶$P < 0.01$; #$P < 0.05$; †$P < 0.05$; symbols identify paired columns for *t* test; bars = S.E.M.).

fat signal dilution [26], fat distribution heterogeneity [27] and blood compared with plasma clearance. Jones et al. [31] and Subramanian et al. [32] also expressed FDG clearance in terms of distribution volume in the lungs in patients with chronic obstructive pulmonary disease, where there are similar problems because of variations in airspace volume in COPD (cf. fat in the liver).

The duration of our dynamic acquisition may be considered limited but longer acquisition periods risk patient movement artefacts, especially in patient volunteers rather than motivated normal volunteers [7–9], and a possible influence of k_4 as intrahepatic FDG-6-P increases, so 30 min seemed reasonable. Others used 40 min [8,9] or 60 min [7].

Physiological hyperinsulinaemia, mediated through an acute glucose load, increases the liver-to-blood FDG concentration ratio in normal subjects [7]. Hepatic steatosis is associated with insulin resistance [10–16]. According to the data of Iozzo et al. [8], k_3, but not k_4, appears unaffected by insulin resistance. Thus, they showed that compared with fasting values, k_3 increased during euglycaemic hyperinsulinaemic clamp in patients with reduced insulin sensitivity as much as in subjects with normal insulin sensitivity. So in insulin resistance, hexokinase is up-regulated as a result of hyperinsulinaemia and increases hepatic glucose clearance. Conversely, glucose-6-phosphatase is insensitive to insulin in insulin resistance. Thus Iozzo et al. [8] found that during hyperinsulinaemia, k_4 was much higher in patients with low insulin sensitivity compared with those with normal or high sensitivity. So in fasting subjects with insulin resistance, k_3 and k_4 are *both* up-regulated. Up-regulation of k_3 is therefore the probable explanation for the increased MRglu of steatosis. An alternative explanation is increased FDG uptake in metabolically active intrahepatic leucocytes in patients with undiagnosed NASH. This is unlikely however because NASH affects only approximately 10% of patients with hepatic steatosis [33], meaning that only two or three patients in our population would have had NASH.

In the only other study we are aware of to measure MRglu in hepatic steatosis by dynamic FDG PET imaging [9], an inverse association between hepatic fat content and glucose utilization was found in patients with type 2 diabetes mellitus, contradicting our findings. However, they measured hepatic FDG concentration in absolute units so total liver volume, against which MRglu was expressed, included fat, which may partly explain this discrepancy. Nevertheless, the range of MRglu they reported is strikingly similar to the range in our five diabetics.

Although obesity is associated with insulin resistance, we found that MRglu was not increased in obese individuals who did not have steatosis. Conversely, non-obese patients with steatosis had increased MRglu. These data show that steatosis, and not obesity *per se,* is associated with increased glucose utilization and probably with insulin resistance.

Non-alcoholic fatty liver disease (NAFLD) is very common and generally thought to be a complication of obesity. It is estimated that the prevalence of NAFLD in Caucasians is approximately 75% in obese subjects [14] and approximately 15% in non-obese subjects [19]. The overall prevalence of obesity is 20–25%, so the prevalence of NAFLD in the general population is approximately 30%. Of our 60 patients, 19 (32%) had steatosis. However, although our patients were not healthy and their numbers small, we found that 42% of these 19 with steatosis were not obese, a rather high value that cannot be attributed to chemotherapy.

In conclusion, hepatic glucose utilization is increased in hepatic steatosis, independently of obesity, probably as a result of insulin resistance, hyperinsulinaemia and up-regulation of hepatic hexokinase.

APPENDIX A

According to the theory of the Patlak–Rutland plot

$$\frac{\mathrm{FDG}\,(t)+\mathrm{FDG6P}\,(t)}{C\,(t)}=\mathrm{Ki}\cdot T+\frac{\mathrm{FDG}\,(t)}{C\,(t)} \tag{1}$$

where FDG and FDG6P are un-phosphorylated and phosphorylated FDG concentrations in the liver, C is FDG concentration in blood and T is normalized time $[\int C(t)\dot{c}dt/C(t)]$. Note that $\mathrm{FDG}(t)/C(t)$ is $V(0)$ and the intercept of the plot.

Re-arranging eqn (1)

$$\frac{\mathrm{FDG6P}\,(t)+\mathrm{FDG}\,(t)}{C\,(t)}-\frac{\mathrm{FDG}\,(t)}{C\,(t)}=\mathrm{Ki}\cdot T \tag{2}$$

Dividing through by $\mathrm{FDG}(t)/C(t)$ [i.e. $V(0)$],

$$\frac{[\mathrm{FDG6P}\,(t)+\mathrm{FDG}\,(t)]/C\,(t)-[\mathrm{FDG}(t)]/C\,(t)}{\mathrm{FDG}\,(t)\,/C\,(t)}=\frac{\mathrm{Ki}\cdot T}{V(0)} \tag{3}$$

Let h and a be the proportionality constants relating hepatic and arterial tracer concentrations to hepatic (H_{FDG} and H_{FDG6P}) and abdominal aortic (A) counts, respectively, then

$$\frac{[h\cdot\{H_{\mathrm{FDG}}\,(t)+H_{\mathrm{FDG6P}}\,(t)\}/a\cdot A\,(t)]-[h\cdot H_{\mathrm{FDG}}\,(t)\,/a\cdot A\,(t)]}{h\cdot H_{\mathrm{FDG}}\,(t)\,/a\cdot A\,(t)}=\frac{Ki\cdot T}{V\,(0)} \tag{4}$$

h and a cancel out so

$$\frac{[\{H_{\mathrm{FDG}}\,(t)+H_{\mathrm{FDG6P}}\,(t)\}/A\,(t)]-[H_{\mathrm{FDG}}\,(t)\,/A\,(t)]}{T\cdot[H_{\mathrm{FDG}}\,(t)\,/A\,(t)]}\,\frac{\mathrm{Ki}}{V(0)} \tag{5}$$

$([\{H_{\mathrm{FDG}}(t)+H_{\mathrm{FDG6P}}(t)\}/A(t)]-[H_{\mathrm{FDG}}(t)/A(t)])T$ is the gradient of the plot based on raw counts and $H_{\mathrm{FDG}}(t)/A(t)$ is the intercept. Therefore, by dividing the gradient by the intercept, ROI of any size can be used for the Patlak–Rutland analysis and there is no need for attenuation correction of either hepatic or abdominal aortic counts.

ETHICAL APPROVAL

All procedures performed in studies involving human participants were in accordance with the ethical standards of the institutional and/or national research committee and with the 1964 Helsinki declaration and its later amendments or comparable ethical standards.

AUTHOR CONTRIBUTION

Georgia Keramida designed the study, and collected and analysed data. James Hunter collected data. Adrien Michael Peters designed the study and analysed data.

REFERENCES

1 Abikhzer, G., Alabed, Y.Z., Azoulay, L., Assayag, J. and Rush, C. (2011) Altered hepatic metabolic activity in patients with hepatic steatosis on FDGPET/CT. Am. J. Roentgenol. **196**, 176–180 CrossRef

2 Lin, C.Y., Lin, W.Y., Lin, C.C., Shih, C.M., Jeng, L.B. and Kao, C.H. (2011) The negative impact of fatty liver on maximum standard uptake value of liver on FDG PET. Clin. Imaging **35**, 437–441 CrossRef PubMed

3 Abele, J.T. and Fung, C.I. (2010) Effect of hepatic steatosis on liver FDG uptake measured in mean standard uptake values. Radiology **254**, 917–924 CrossRef PubMed

4 Kamimura, K., Nagamachi, S., Wakamatsu, H., Higashi, R., Ogita, M., Ueno, S., Fujita, S., Umemura, Y., Fujimoto, T. and Nakajo, M. (2010) Associations between liver (18)F fluoro-2-deoxy-D-glucose accumulation and various clinical parameters in a Japanese population: influence of the metabolic syndrome. Ann. Nucl. Med. **24**, 157–161 CrossRef PubMed

5 Bural, G.G., Torigian, D.A., Burke, A., Houseni, M., Alkhawaldeh, K., Cucchiara, A., Basu, S. and Alavi, A. (2010) Quantitative assessment of the hepatic metabolic volume product in patients with diffuse hepatic steatosis and normal controls through use of FDG-PET and MR imaging: a novel concept. Mol. Imaging Biol. **12**, 233–239 CrossRef PubMed

6 Hong, S.P., Noh, T.S., Moon, S.H., Cho, Y.S., Lee, E.J., Choi, J.Y., Kim, B.T. and Lee, K.H. (2014) Hepatic glucose uptake is increased in association with elevated serum γ-glutamyl transpeptidase and triglyceride. Dig. Dis. Sci. **59**, 607–613 CrossRef PubMed

7 Choi, Y., Hawkins, R.A., Huang, S.C., Brunken, R.C., Hoh, C.K., Messa, C., Nitzsche, E.U., Phelps, M.E. and Schelbert, H.R. (1994) Evaluation of the effect of glucose ingestion and kinetic model configurations of FDG in the normal liver. J. Nucl. Med. **35**, 818–823 PubMed

8 Iozzo, P., Geisler, F., Oikonen, V., Mäki, M., Takala, T., Solin, O., Ferrannini, E., Knuuti, J., Nuutila, P., 18F-FDG PET Study. (2003) Insulin stimulates liver glucose uptake in humans: an ^{18}F-FDG PET Study. J. Nucl. Med. **44**, 682–689 PubMed

9 Borra, R., Lautamäki, R., Riitta Parkkola, R., Komu, M., Sijens, P.E., Hällsten, K., Bergman, J., Iozzo, P. and Nuutila, P. (2008) Inverse association between liver fat content and hepatic glucose uptake in patients with type 2 diabetes mellitus. Metab. Clin. Exp. **57**, 1445–1451 CrossRef PubMed

10 Deivanayagam, S., Mohammed, B.S., Vitola, B.E., Naguib, G.H., Keshen, T.H., Kirk, E.P. and Klein, S. (2008) Nonalcoholic fatty liver disease is associated with hepatic and skeletal muscle insulin resistance in overweight adolescents. Am. J. Clin. Nutr. **88**, 257–262 PubMed

11 González-Périz, A., Horrillo, R., Ferré, N., Gronert, K., Dong, B., Morán-Salvador, E., Titos, E., Martínez-Clemente, M., López-Parra, M., Arroyo, V. and Clària, J. (2009) Obesity-induced insulin resistance and hepatic steatosis are alleviated by omega-3 fatty acids: a role for resolvins and protectins. FASEB J. **23**, 1946–1957 CrossRef PubMed

12 Marchesini, G., Brizi, M., Morselli-Labate, A.M., Bianchi, G., Bugianesi, E., McCullough, A.J., Forlani, G. and Melchionda, N. (1999) Association of nonalcoholic fatty liver disease with insulin resistance. Am. J. Med. **107**, 450–455 CrossRef PubMed

13 Garg, A. and Misra, A. (2002) Hepatic steatosis, insulin resistance, and adipose tissue disorders. J. Clin. Endocrinol. Metab. **87**, 3019–3022 CrossRef PubMed

14 Farrell, G.C. and Larter, C.Z. (2006) Nonalcoholic fatty liver disease: from steatosis to cirrhosis. Hepatology **43** (2 Suppl. 1), S99–S112 CrossRef PubMed

15 Abdelmalek, M.F. and Diehl, A.M. (2007) Nonalcoholic fatty liver disease as a complication of insulin resistance. Med. Clin. North Am. **91**, 1125–1149 CrossRef PubMed
16 Postic, C. and Girard, J. (2008) Contribution of *de novo* fatty acid synthesis to hepatic steatosis and insulin resistance: lessons from genetically engineered mice. J. Clin. Invest. **118**, 829–838 CrossRef PubMed
17 Shanik, M.H., Xu, Y., Skrha, J., Dankner, R., Zick, Y. and Roth, J. (2008) Insulin resistance and hyperinsulinemia: is hyperinsulinemia the cart or the horse? Diabetes Care **31** (Suppl. 2), S262–S268 CrossRef PubMed
18 Kanda, H., Tateya, S., Tamori, Y., Kotani, K., Hiasa, K., Kitazawa, R., Kitazawa, S., Miyachi, H., Maeda, S., Egashira, K. and Kasuga, M. (2006) MCP-1 contributes to macrophage infiltration into adipose tissue, insulin resistance, and hepatic steatosis in obesity. J. Clin. Invest. **116**, 1494–1505 CrossRef PubMed
19 Venturi, C., Zoppini, G., Zamboni, C. and Muggeo, M. (2004) Insulin sensitivity and hepatic steatosis in obese subjects with normal glucose tolerance. Nutr. Metab. Cardiovasc. Dis. **14**, 200–204 CrossRef PubMed
20 Bellentani, S., Saccoccio, G., Masutti, F., Crocè, L.S., Brandi, G., Sasso, F., Cristanini, G. and Tiribelli, C. (2000) Prevalence of and risk factors for hepatic steatosis in Northern Italy. Ann. Intern. Med. **132**, 112–117 CrossRef PubMed
21 Keramida, G., Dunford, A., Siddique, M., Cook, G.J. and Peters, A.M. (2016) Relationships of body habitus and SUV indices with signal-to-noise ratio of hepatic ^{18}F-FDG PET. Eur. J. Radiol. **85**, 1012–1025 CrossRef PubMed
22 Boyce, C.J., Pickhardt, P.J., Kim, D.H., Taylor, A.J., Winter, T.C., Bruce, R.J., Lindstrom, M.J. and Hinshaw, J.L. (2010) Hepatic steatosis (fatty liver disease) in asymptomatic adults identified by unenhanced low-dose CT. Am. J. Roentgenol. **194**, 623–628 CrossRef
23 Keiding, S., Munk, O.L., Schiøtt, K.M. and Hansen, S.B. (2000) Dynamic 2-[^{18}F]fluoro-2-deoxy-D-glucose positron emission tomography of liver tumours without blood sampling. Eur. J. Nucl. Med. **27**, 407–412 CrossRef PubMed
24 de Geus-Oei, L.F., Visser, E.P., Krabbe, P.F., van Hoorn, B.A., Koenders, E.B., Willemsen, A.T., Pruim, J., Corstens, F.H. and Oyen, W.J. (2006) Comparison of image-derived and arterial input functions for estimating the rate of glucose metabolism in therapy-monitoring ^{18}F-FDG PET studies. J. Nucl. Med. **47**, 945–949 PubMed
25 Munk, O.L., Bass, L., Roelsgaard, K., Bender, D., Hansen, S.B. and Keiding, S. (2001) Liver kinetics of glucose analogs measured in pigs by PET: importance of dual-input blood sampling. J. Nucl. Med. **42**, 795–801 PubMed
26 Keramida, G., Potts, J., Bush, J., Verma, S., Dizdarevic, S. and Peters, A.M. (2014) Accumulation of ^{18}F-fluorodeoxyglucose in the liver in hepatic steatosis. Am. J. Roentgenol. **203**, 643–648 CrossRef
27 Decarie, P.O., Lepanto, L., Billiard, J.S., Olivié, D., Murphy-Lavallée, J., Kauffmann, C. and Tang, A. (2011) Fatty liver deposition and sparing: a pictorial review. Insights Imaging **2**, 533–538 CrossRef PubMed
28 Iozzo, P., Jarvisalo, M.J., Kiss, J., Borra, R., Naum, G.A., Viljanen, A., Viljanen, T., Gastaldelli, A., Buzzigoli, E., Guiducci, L. et al. (2007) Quantification of liver glucose metabolism by positron emission tomography: validation study in pigs. Gastroenterology **132**, 531–542 CrossRef PubMed
29 Tragardh, M., Moller, N. and Sorensen, M. (2015) Methodologic considerations for quantitative ^{18}F-FDGPET/CT studies of hepatic glucose metabolism in healthy subjects. J. Nucl. Med. **56**, 1366–1371 CrossRef PubMed
30 Nahmias, C., Wahl, L.M., Amano, S., Asselin, M.C. and Chirakal, R. (2000) Equilibration of 6-[18F]fluoro-L-m-tyrosine between plasma and erythrocytes. J. Nucl. Med. **41**, 1636–1641 PubMed
31 Jones, H.A., Marino, P.S., Shakur, B.H. and Morrell, N.W. (2003) *In vivo* assessment of lung inflammatory cell activity in patients with COPD and asthma. Eur. Respir. J. **21**, 567–573 CrossRef PubMed
32 Subramanian, D.R., Jenkins, L., Edgar, R., Quraishi, N., Stockley, R.A. and Parr, D.G. (2012) Assessment of pulmonary neutrophilic inflammation in emphysema by quantitative positron emission tomography. Am. J. Respir. Crit. Care Med. **186**, 1125–1132 CrossRef PubMed
33 Bellentani, S., Scaglioni, F., Marino, M. and Bedogni, G. (2010) Epidemiology of non-alcoholic fatty liver disease. Dig. Dis. **28**, 155–161 CrossRef PubMed

Received 2 September 2016/15 September 2016; accepted 21 September 2016

Accepted Manuscript online 21 September 2016, doi 10.1042/BSR20160381